Analytical Model for Photocurrent in Organic Solar Cells as a Function of the Charge-Transport Figure of Merit Including Second-Order Recombination

Daniel R.B. Amorim,[1] Douglas J. Coutinho,[2] Paulo B. Miranda,[1] and Roberto M. Faria[1,*]

[1] *Instituto de Física de São Carlos, Universidade de São Paulo, P.O. Box 369, São Carlos – São Paulo, 13560-970, Brazil*

[2] *Federal University of Technology – Paraná (UTFPR), Toledo – Paraná, 85902-490, Brazil*

(Received 4 November 2019; revised 11 May 2020; accepted 10 July 2020; published 17 September 2020)

We develop an analytical model for the photocurrent of organic solar cells based on carrier drift and including second-order charge recombination, in which the figure of merit θ_o naturally appears. This approach provides expressions for the fill-factor–θ_o and α-θ_o relations, where α is the exponent of the function of the short-circuit current versus light intensity ($J_{SC} \propto I^{\alpha}$). A correlation between the reduction factor of Langevin recombination and the dissociation probability of charge transfer states (P) is also discussed. Photocurrent curves of a polymer device obtained at different temperatures (100–300 K) are fitted by the model, whose fitting parameters are in agreement with the literature.

DOI: 10.1103/PhysRevApplied.14.034046

I. INTRODUCTION

After more than 70 years of continuous study, since the pioneering work on semiconductor photovoltaic devices [1] to the recent organic layered cells of nanometer thicknesses [2,3], significant gaps in fundamental understanding of the current-voltage (J-V) photovoltaic response still persist [4]. Numerous studies devoted to efficiency losses of organic solar cells have emphasized the crucial role of charge extraction and recombination rates in the device performance, in either short-circuit or open-circuit conditions [4–7]. The seminal paper on solar-cell efficiency, written in 1961 by Shockley and Queisser [8], still serves as a beacon for the solar cells now under investigation, especially for bulk heterojunction organic solar cells (BHJ OSCs). It was the first setting a limit on the efficiency of solar cells, besides deducing a relationship between the fill factor (FF) and the open-circuit voltage (V_{OC}). In organic solar cells, a conclusive understanding of concepts behind the FF is still a matter of debate [9–13], and a deep understanding of the whole process of generation, recombination, and extraction of charge carriers is essential to increase the efficiency of modern photovoltaic devices.

Recently, Bartesaghi *et al.* [12] revealed, by drift-diffusion numerical simulations, a relationship between the FF and a single figure of merit θ, which quantifies the competition among charge generation, extraction and recombination. This FF-θ relation was successfully used by Heiber *et al.* [13] to fit results from impedance-photocurrent device analysis obtained with different organic devices. However, the figure of merit fails for Langevin systems when space-charge effects cannot be ignored [14]. Later, Würfel *et al.* [4] adapted the standard Shockley diode equation for low-mobility organic solar cells by introducing a current-dependent internal voltage, and considering bimolecular recombination. They demonstrated that such a modified Shockley equation could describe well simulated J-V curves based on a one-dimensional drift-diffusion model, for a wide parameter range. The same group [15] demonstrated that this modified Shockley model can be related to the same figure of merit θ, arriving at an analytical expression for the photocurrent of organic solar cells that involves the parameter θ. They also proposed, on the basis of expressions for inorganic (high mobility) solar cells, an empirical relation between the FF and θ. Other authors have also attempted to derive analytical expressions for the photocurrent of organic solar cells based on carrier drift diffusion, but they assumed either first-order recombination [16] or bimolecular recombination with a constant charge density (constant carrier lifetime) [17]. Set *et al.* [18] used scaling analysis of a drift-diffusion model with bimolecular recombination to obtain implicit equations that yields J-V curves, predicting the intensity dependence of the photocurrent ($J_{SC} \propto I^{\alpha}$), but they do not provide explicit expressions for the dependence of the FF or α on the figure of merit θ.

In this paper we present a derivation of an analytical expression for photocurrent curves (J_{ph}-V) applied to a bulk heterojunction device based on carrier drift, assuming second-order kinetics for the bimolecular recombination, in which a figure of merit θ_o naturally appears. From the theoretical expression for the maximum power,

*faria@ifsc.usp.br

we derive a relation for the FF as a function of θ_o, which reproduces the same trend as obtained by Bartesaghi *et al.* [12] from numerical simulations, but with the additional hypothesis of equal carrier mobilities. The factor α, the exponent of the relationship between the short-circuit current and the incident light intensity on the device ($J_{SC} \propto I^{\alpha}$), is discussed in the literature as a factor associated with the type of bimolecular recombination [19–22]. Here a relation between α and θ_o is also derived from our model, which assumes only second-order recombination. Finally, we fit J_{ph}-V measurements obtained at various temperatures on a standard ITO/poly(3,4-ethylenedioxythiophene) (PEDOT):polystyrene sulfonate (PSS)/poly(3-hexylthiophene) (P3HT):[6,6]-phenyl-C_{61}-butyric acid methyl ester (PC61BM)/Ca/Al device using our photocurrent expression. From the fittings, we obtain the temperature dependence of the charge-carrier mobility (μ) and the charge-transfer- (CT) state dissociation coefficient (P), in good agreement with experimental data. We further associate P with the recombination coefficient reduction factor (ζ).

II. EXPERIMENTAL

The devices used in the experimental part of this work are BHJ OSCs having the following structure: ITO/PEDOT:PSS/regioregular P3HT (rrP3HT):$PC_{61}BM$ (1:1, w/w)/Ca/Al (Fig. 1). Both rrP3HT and $PC_{61}BM$ (99.5% purity) are purchased from Aldrich and used as received. A high-pressure-size-exclusion-chromatography technique is used to obtain the molar masses of rrP3HT ($M_n = 22$ kDa, $M_w = 36$ kDa), as well as the polydispersity index (1.6), measured with 1 ml tetrahydrofuran per minute at 35 °C as the eluent in an Agilent 1100 chromatographic system with a refractive-index detector, in two PLgel mixed columns and polystyrene standards. Proton NMR spectroscopy in a $CDCl_3$ solution with a Bruker 400-MHz spectrometer is used to determine the degree of regioregularity, which is found to be 93%. Glass coated with ITO substrates (Delta Technologies) is cleaned with detergent, sonicated in acetone and hot isopropyl alcohol, and dried under nitrogen flow before being exposed to UV–ozone treatment for 10 min. PEDOT:PSS (Clevios P), used as hole transport layer, is spin-cast at 3000 revolutions/min for 1 min to form films of approximately-40-nm thickness. This film is then annealed for 10 min at 120 °C in an inert atmosphere. A solution of rrP3HT:$PC_{61}BM$ (1:1 by weight) in dichlorobenzene (40 mg/ml) is stirred for 24 h at 60 °C before deposition, and is spin-cast at 700 revolutions/min for 3 min on top of the PEDOT:PSS film, forming a layer approximately 285 nm thick (measured by a Veeco Dektak 150 profilometer). The device's performance is improved by thermal annealing performed at 140 °C for 5 min on a hotplate. Finally, a top electrode made of calcium (40 nm) and aluminium (70 nm) is thermally evaporated through a shadow mask under low pressure (10^{-6} mbar). Six similar devices are prepared in the same batch, all of them exhibiting very similar electrical responses. Current-voltage (J-V) measurements are performed in a custom-made sample holder designed to keep the devices under a nitrogen atmosphere or in a cryostat for measurements performed at different temperatures. For the J-V measurements, a Keithley 2400 source measurement unit is used, and illumination is provided by an AM1.5G simulator (100 mW/cm^2) using a xenon-lamp-based solar simulator (Thermo Oriel 66921, 450 W). The different light-irradiation intensities are obtained with a set of neutral-density optical filters. The technique of photoinduced-charge-carrier extraction by linearly increasing voltage (photo-CELIV), used here to measure the charge-carrier mobility, uses a N_2-pumped MNL 100 dye laser (LTB Laser technik Berlin) with a wavelength of 590 nm and a pulse duration of 3 ns.

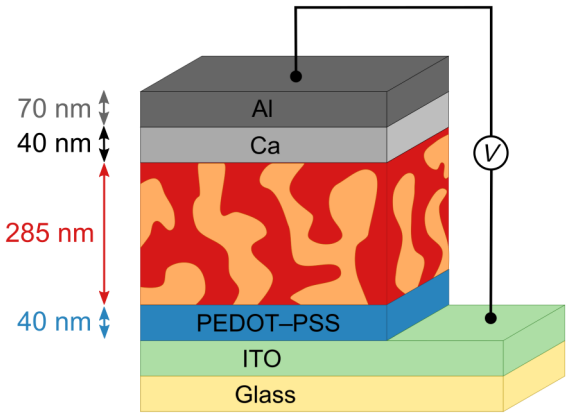

FIG. 1. Structure of the ITO/PEDOT:PSS/P3HT:PC61BM/Ca/Al BHJ-OSC device.

III. MODEL

Figure 2 shows a simplified scheme of the electronic structure of a classic BHJ OSC, in the dark and without any space charge, in which the transport layers are incorporated in the electrodes. In this picture the energy of the forbidden gap E_G is the result of the difference between the LUMO of the acceptor and the HOMO of the donor. Thereby, we can see that the built-in voltage V_{bi} is given by the difference between the energy of the gap E_G and the potential barriers $\Delta\phi_p$ and $\Delta\phi_n$ of the anode and the cathode, respectively. Eventually, the barriers $\Delta\phi_p$ and $\Delta\phi_n$ may be null, and then we can simply take $eV_{bi} = E_G$. The magnitude of the electric field F is given by $(V_{bi} - V)/L$, and by taking $eV_{bi} = E_G$, this means that we are ignoring any polarization effect at interfaces with the electrodes, assuming quasi-Ohmic contacts, so that charge carriers at the interfaces are totally collected by the electrodes. We

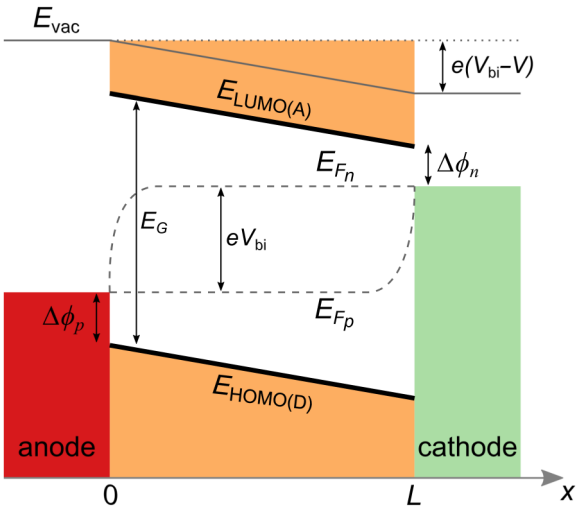

FIG. 2. Electronic structure of a BHJ organic solar cell. A, acceptor; D, donor.

also assume, for simplicity and with a small error, that light absorption is uniform across the active layer.

The model to be developed is based on the electronic structure scheme shown in Fig. 2, in which the active layer falls within the scope of low-mobility semiconductors (π-conjugated polymers), and it is also assumed that recombination between opposite-charge carriers obeys a bimolecular process controlled by second-order kinetics following the diffusion-controlled model developed by Langevin [23]. In this model, the recombination is given by $R = \gamma_L np$, where $\gamma_L = (e/\varepsilon\varepsilon_0)(\mu_n + \mu_p)$. Despite it being well accepted that charge-carrier-recombination mechanism in BHJ OSCs follows the Langevin model, experimental results have revealed that the recombination coefficient can be orders of magnitude smaller than the Langevin coefficient (i.e., $\gamma \ll \gamma_L$) [24–26]. Several models have tried to explain the reduction factor (ζ) by invoking charge-transfer phenomenon at donor-acceptor interfaces existing inside the complex active-layer morphology [27–31]. That is, the number of free photogenerated carriers comes from the dissociation of the CT state formed at the donor-acceptor interface [32], which is then determined by the product GP, where G is the generation rate of CT states and P is the dissociation coefficient. Following the Braun-Onsager model [33], P can be temperature and electric field dependent. Moreover, it is important to remark that it has been shown that P in BHJ OSCs is practically independent of the electric field up to fields of a few tens of kilovolts per centimeter [34,35], also shown by incoherent-hopping mechanisms [36,37]. There is an additional term for the charge-generation rate due to CT-state "failure to recombine" that is given by RP. Driven by the internal field, set by the built-in voltage (V_{bi}), the free charge carriers can be either extinguished by recombination or collected by the electrodes. This description follows the same principles that were used by Koster *et al.* [38], among others [39,40].

In solar cells composed of very thin films as the BHJ OSCs, the current densities of electrons and holes are generally given by drift and diffusion components:

$$J_n = e\left(n\mu_n F + D_n \frac{\partial n}{\partial x}\right), \tag{1}$$

$$J_p = e\left(p\mu_p F - D_p \frac{\partial p}{\partial x}\right),$$

where μ_n (μ_p)and D_n (D_p) are the mobility and diffusion coefficient of electrons (holes), F is the electric field, n (p) the density of electrons (holes), and e is the elementary charge. J_n and J_p above are taken as the magnitude of the photocurrent, and are therefore positive. In numerous studies, it has been observed that the mobility values of both carriers are very similar [41,42], and this is assumed throughout this paper. Assuming then not very disparate values of electron and hole mobilities, we replace them by the square-root mobility $\mu = \sqrt{\mu_n \mu_p}$, as has been used by other authors [11]. The relative importance of diffusion effects can be estimated from the ratio between the diffusion current and the drift current, given approximately by $D_n(n/L)/nF\mu = V_t/FL = V_t/(V_{bi} - V)$, where we use the Einstein relation for diffusion ($D/\mu = kT/e = V_t$). At room temperature, for instance, V_t is approximately 25 mV, and by considering $V_{bi} \sim V_{OC} = 0.6$ V, we can see that the diffusion and drift currents are comparable only very close to V_{OC} (within V_t of V_{OC}), as assumed in the model. The prevalence of the drift current over the diffusion current is also supported by results and considerations found in other work [43,44]. Thereby, general expressions for the continuity equations for electrons and holes, including the generation and recombination mechanisms, are given by

$$\begin{aligned}\frac{\partial n}{\partial t} &= GP - R + RP - \mu F \frac{\partial n}{\partial x} \\ &= GP - (1-P)\gamma_L np - \mu F \frac{\partial n}{\partial x},\end{aligned} \tag{2}$$

$$\begin{aligned}\frac{\partial p}{\partial t} &= GP - R + RP + \mu F \frac{\partial p}{\partial x} \\ &= GP - (1-P)\gamma_L np + \mu F \frac{\partial p}{\partial x}.\end{aligned}$$

In steady-state conditions, these simplify to

$$\begin{aligned}\mu F \frac{\partial n}{\partial x} &= GP - (1-P)\gamma_L np, \\ -\mu F \frac{\partial p}{\partial x} &= GP - (1-P)\gamma_L pn.\end{aligned} \tag{3}$$

In the expressions in Eq. (3), we assume that $(1-P)\gamma_L$ is a new recombination coefficient γ, where $(1-P)$ contributes to reduce the Langevin coefficient. Also, from the equality in the expressions in Eq. (3), one easily verifies that the sum $n(x)+p(x)=C$, where C is a constant (see Fig. S3 in Supplemental Material [45]). This result is valid for almost the entire active layer, except for the thin interfacial regions near the electrodes, where the diffusion current is not negligible. Then, replacing p by $(C-n)$ in the expressions in Eq. (3), we have

$$\frac{dn}{dx} = \phi n^2 + \beta n + \chi, \tag{4}$$

where $\phi = \gamma/\mu F$, $\beta = -\gamma C/\mu F$, and $\chi = GP/\mu F$. A similar expression is obtained for dp/dx [Eq. (A18) in Supplemental Material [45]]. This type of differential equation is known as the Riccati differential equation [46], whose solution is obtained by applying the method used by Lorrmann *et al.* [47]. With substitution of variables, the variable n is replaced by N, so $dN/dx = -\phi n N$. Once n is now a function of N and dN/dx, a new homogeneous second-order ordinary differential equation is obtained, whose solution (see Supplemental Material [45] for details) gives $n(x)$ [and $p(x)$, from the corresponding equation for dp/dx] [45]:

$$\begin{aligned} n(x) &= -\frac{1}{\phi}\frac{[\exp(D_1 x) - \exp(D_2 x)]}{\left[\frac{1}{D_1}\exp(D_1 x) - \frac{1}{D_2}\exp(D_2 x)\right]}, \\ p(x) &= -\frac{1}{\phi}\frac{\{\exp[D_1(L-x)] - \exp[D_2(L-x)]\}}{\left\{\frac{1}{D_1}\exp[D_1(L-x)] - \frac{1}{D_2}[\exp[D_2(L-x)]]\right\}}. \end{aligned} \tag{5}$$

In these solutions, $D_1 = \beta/2 + \sqrt{(\beta/2)^2 - \phi\chi}$ and D_2 $D_2 = \beta/2 - \sqrt{(\beta/2)^2 - \phi\chi}$ are set by our taking the boundary conditions $n(0)=0$ for $x=0$, and $p(L)=0$ for $x=L$. These boundary conditions stem from the drift due to the internal field, which drives electrons toward the cathode ($x=L$) and holes toward the anode ($x=0$). Thus, assuming that they are not collected at the opposite electrodes, we set $n(0)=0$ and $p(L)=0$. Since Eq. (4) is first order in n, only one boundary condition suffices for each carrier, with the charge density at the collecting electrode free to vary due to generation, drift and recombination. The equal values for the electron and hole mobilities lead to perfect symmetry for the $n(x)$ and $p(x)$ distributions. Assuming that $L\sqrt{\phi\chi - (\beta/2)^2} \lesssim 1$ (see Supplemental Material [45] for a discussion), the expressions in Eq. (5) can be simplified to

$$\begin{aligned} n(x) &= \frac{2GPx}{2\mu F + (1-P)\gamma_L C x}, \\ p(x) &= \frac{2GP(L-x)}{2\mu F + (1-P)\gamma_L C(L-x)}. \end{aligned} \tag{6}$$

Knowing the value of $C=2n(x)$, obtained at the midpoint $x=L/2$ of the active layer, we finally obtain the expression for the resulting magnitude of the photocurrent [$J_{\rm ph} = eC\mu F$, from Eq. (1)]:

$$J_{\rm ph} = 2eGPL\frac{\left(1 - \frac{V}{V_{\rm bi}}\right)^2}{\theta_o}\left[\sqrt{1 + \frac{\theta_o}{\left(1 - \frac{V}{V_{\rm bi}}\right)^2}} - 1\right], \tag{7}$$

where

$$\theta_o = \frac{GPL^4(1-P)\gamma_L}{(\mu V_{\rm bi})^2}. \tag{8}$$

In the limit that $P \to 1$ (i.e., for the case where one CT state gives rise to a free electron-hole pair), $J_{\rm ph} \to eGL$, and when $P \to 0$, the photocurrent tends to zero, as expected. This intriguing physical parameter θ_o, introduced by Bartesaghi *et al.* [12], now slightly modified by the inclusion of the dissociation probability P, represents the competition between the fundamental process of the photovoltaic cell: generation (G), recombination (γ_L), and extraction (μ). Bartesaghi *et al.* also obtained a sigmoidal curve for the FF dependence on the logarithm of this parameter, whose shape was obeyed by more than 15 BHJ solar cells whose data were obtained from the literature [12]. To ensure the validity of Eq. (7), we simulate $J_{\rm ph}$-V curves by using this equation and also the numerical model developed by Koster *et al.* [38], using the same physical parameters (mobility, recombination coefficient, and dissociation probability P). In item B in Supplemental Material, we show some profile curves of $n(x)$ and $p(x)$ obtained from both simulations (Fig. S2) [45]; the profiles are quite coincident at $J_{\rm SC}$ and at the FF point, disagreeing near $V_{\rm OC}$ as expected due to the dominance of the diffusion current.

IV. FILL FACTOR, EXPONENT α, AND FIGURE-OF-MERIT PARAMETER

The FF has a major influence on the solar-cell power-conversion efficiency, but it is not yet well understood despite numerous studies of the performance of solar cells since the seminal paper of Shockley and Queisser [8]. Starting from the photocurrent expression [Eq. (7)], we derive how the FF varies with θ_o (calculations in Supplemental Material [45]), whose results are given by the

expressions

$$FF = \frac{v(1-v)^3}{(2v-1)\left[\sqrt{1+\theta_o}-1\right]} \tag{9}$$

and

$$\theta_o = \frac{(1-v)^3(3v-1)}{(2v-1)^2}, \tag{10}$$

where $v = V_{\max}/V_{\text{bi}}$, and $V_{\max}$ is the output voltage at the maximum-power point. The FF-θ_o plot is in agreement with the sigmoidal pattern numerically simulated by Bartesaghi *et al.* [12], as shown in Fig. 3; also θ_o as a function of v is shown in Fig. S4 [45].

According to the limit of high electric field in Eq. (7), the short-circuit current J_{SC} is equal to $eGPL$ (saturated photocurrent); therefore, J_{SC} is proportional to G, and then $J_{\text{SC}} \propto I$. On the other hand, when the internal field is too low, the photocurrent tends to $2e\mu F\sqrt{GP/(1-P)\gamma_L}$, resulting in J_{SC} being proportional to $G^{1/2}$. Thereby, from the J_{ph}-V model described above, the variation of the exponent α between 0.5 and 1 is fully compatible with second-order kinetics for bimolecular recombination, and is due simply to operating regimes where the charge extraction is slower or faster than charge recombination, respectively. Figure 4 shows simulations of J_{SC}-I curves, for different relative values of charge-carrier mobility, which simulate good performance of a solar cell (mobility μ, corresponding to $\theta_o < 10^{-1}$) and bad performance (mobility $\mu/100$, corresponding to $\theta_o > 10^2$).

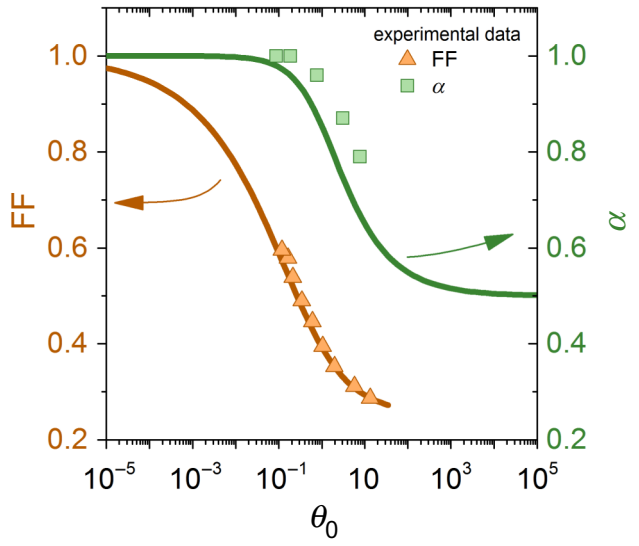

FIG. 3. FF-θ_o curve obtained from the plot of Eqs. (9) and (10) (orange line, left axis), and α-θ_o curve obtained from Eq. (11) (green line, right axis); experimental points extracted from measurements on a ITO/PEDOT:PSS/P3HT:PC61BM/Ca/Al device obtained at different temperatures (from 100 to 300 K) are shown to coincide well with the predicted curves.

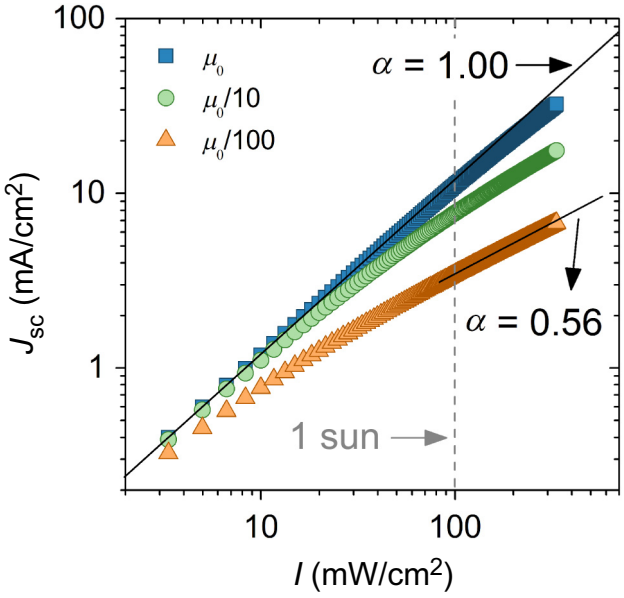

FIG. 4. Simulated curves of short-circuit current versus light intensity ($J_{\text{SC}} \propto I^{\alpha}$), from Eq. (7).

Finally, still from Eq. (7) we derive a relationship between the exponent α and the factor θ_o, given by Eq. (11) (details in Supplemental Material [45]), whose result is also plotted in Fig. 3:

$$\alpha = \frac{1}{2\left[1-\frac{1}{\theta_o}\left(\sqrt{1+\theta_o}-1\right)\right]}. \tag{11}$$

This $\alpha(\theta_o)$ expression shows that α is equal to 1 for θ_o values lower than 10^{-1}, decreasing in value as θ_o increases, tending to 1/2 for $\theta_o > 10^2$.

V. APPLICATION TO A P3HT:PC$_{61}$BM DEVICE

We then use Eq. (7) to fit J_{ph}-V measurements obtained in an ITO/PEDOT:PSS/P3HT:PC61BM/Ca/Al solar cell at different temperatures. The device manufacturing processes are described elsewhere [48], and follow the standard procedure used in most of these types of solar cells. Isothermal measurements are performed from 100 to 300 K, and while the short-circuit current and the fill factor significantly increase as the temperature increases, the open-circuit voltage decreases slightly, as shown in Fig. 5(a). Once G is a relatively well determined value for organic solar cells (in general about 10^{21} cm^{-3} s^{-1}), the shape of the J-V curve depends strongly on θ_o, while P has an influence on the amplitude of the photocurrent. In the short-circuit condition ($V = 0$), Eq. (7) reduces to $J_{SC} = 2eGPL(1/\theta_o)\left(\sqrt{1+\theta_o}-1\right)$, and for good solar cells ($\theta_o \ll 1$) it approaches the saturation current, which

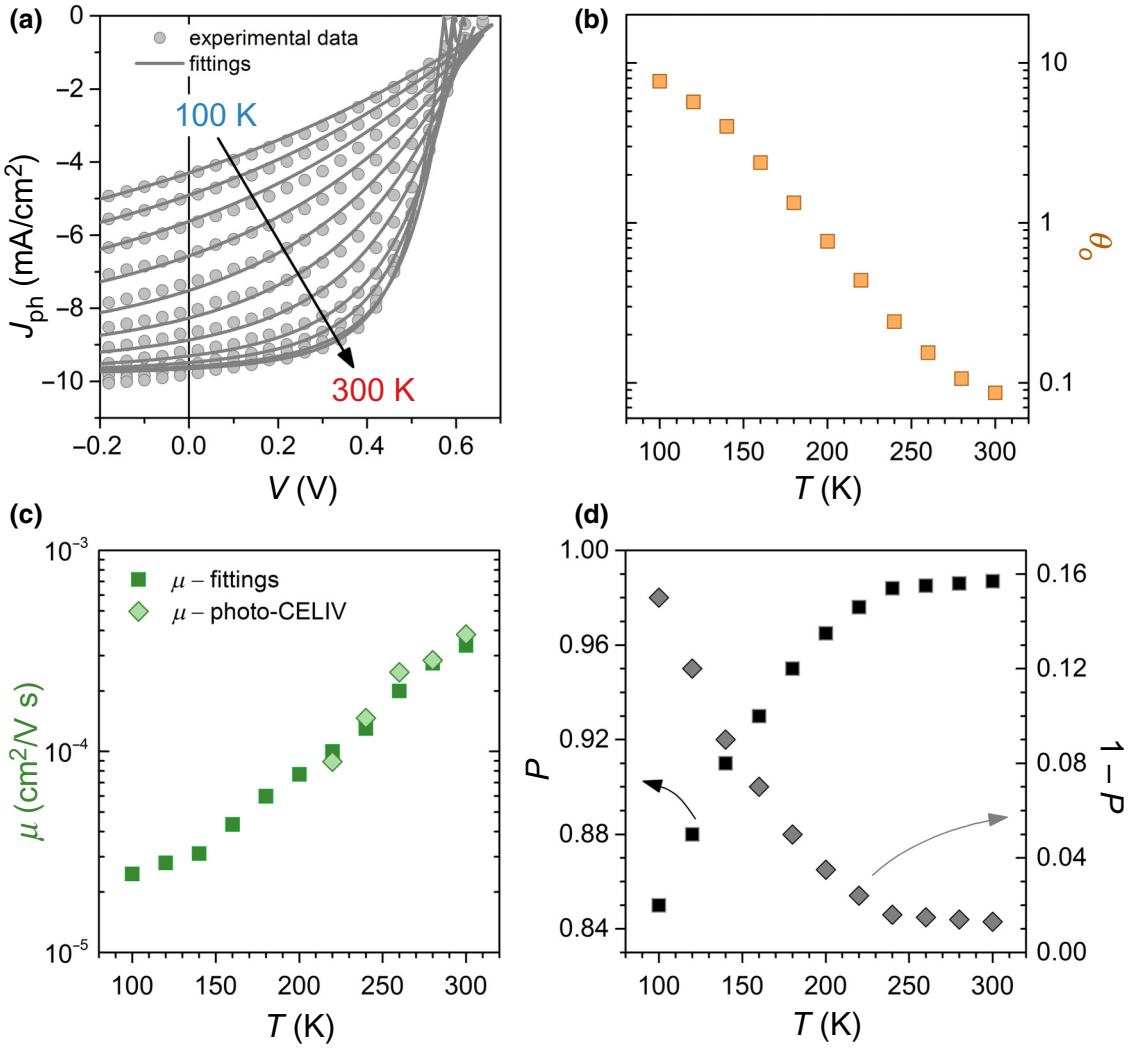

FIG. 5. (a) J-V measurements of an ITO/PEDOT:PSS/P3HT:PC61BM/Ca/Al device for different temperatures (gray circles) and fittings using Eq. (7) (solid gray lines); (b) θ_o versus T, (c) μ versus T, and (d) P and $1-P$ versus T are obtained from the fittings as adjusted parameters.

is given by $J_{sat} = eGPL$. Therefore, θ_o and P can be obtained directly from the J_{ph}-V fittings shown in Fig. 5(a). Figure 5(b) shows the adjusted values of θ_o; values of θ_o from this curve are also displayed in the FF-θ_o curve (Fig. 3). Figure 5(d) shows the temperature dependence of P, and $1-P$, which is also obtained independently of θ_o from the fits to Eq. (7), since θ_o largely determines the shape of the J-V curve, while an additional factor P appears in the saturation current. Here we consider $1-P$ as part of the reduction factor of the recombination coefficient (ζ). As a test of the model, the temperature dependence of the mobilityμ [Fig. 5(c)] is extracted from the fitted values of P and θ_o by use of Eq. (8) and by taking into account that $\gamma = (1-P)\gamma_L$, with the Langevin recombination coefficient expressed in terms of the mobility, $\gamma_L \approx 2e\mu/\varepsilon\varepsilon_o$, and taking the active-layer dielectric constant $\varepsilon = 3.5$. The light-green diamonds in the mobility curve [Fig. 5(c)], displayed between 225 and 300 K, are mobility values obtained directly from photo-CELIV measurements, which match very well the mobilities obtained from the fitted values of P and θ_o by use of $\gamma = (1-P)\gamma_L$ as described above. Photo-CELIV measurements at lower temperatures are not possible because the current transients become too wide in the duration of the voltage ramp (tens of microseconds). The dependence of mobility on temperature shown in Fig. 5(c) is consistent with other reports [49,50]. The value of the dissociation probability P at room temperature is in agreement with that evaluated in other articles [48–51] and its temperature dependence follows well the model presented by Braun [33].

Lastly, Fig. 6 shows the dependence of the short-circuit current on the light intensity incident on the ITO/PEDOT:PSS/P3HT:PC61BM/Ca/Al device between 0.1 and 1 sun (100 mW/cm^2), whose measurements are

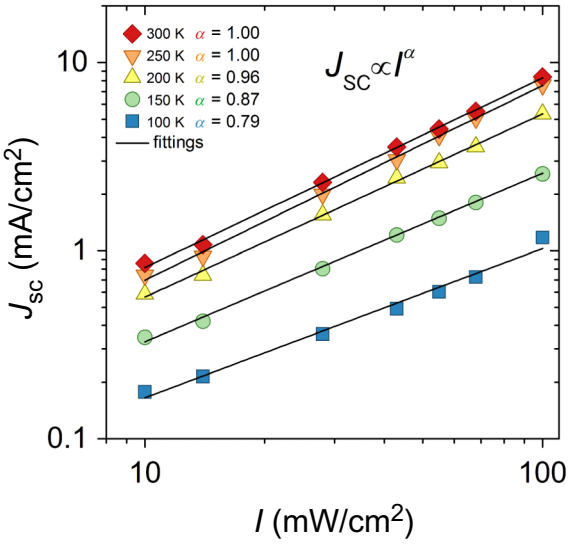

FIG. 6. Short-circuit current versus light intensity obtained from measurements performed with an ITO/PEDOT:PSS/P3HT:PC61BM/Ca/Al device for different temperatures, where the relation $J_{SC} \propto I^{\alpha}$ is obeyed.

performed at different temperatures from 100 to 300 K. At room temperature this dependence is linear, becoming increasingly sublinear as the temperature decreases, reaching the relation $J_{SC} \propto I^{0.79}$ at 100 K. The values of α obtained from the measurements in Fig. 6 are plotted in Fig. 3, in the α-θ_o curve. The fact that the α values are obtained by varying the light intensity and θ_o under 1 sun may explain the slight deviation from the theoretical prediction, especially at lower temperatures. Until a few years ago it was well accepted that the linear case, $\alpha = 1$, would indicate that the electronic transport process involves first-order kinetics for the recombination of the photogenerated carriers, while α values less than 1 are the result of second-order recombination [20,52]. However, some publications have shown that this assertion is not so reliable [53,54], indicating that $\alpha = 1$ is a result of negligible recombination effects instead of first-order kinetics. This is demonstrated here by the limits of strong and weak electric fields in Eq. (7).

VI. CONCLUSIONS

In summary, we derive a simple analytical equation for the current-voltage curve of BHJ OSCs, in which the factor θ_o, which represents the competition among charge generation, extraction, and recombination, arises as an important physical parameter. The model assumes second-order bimolecular recombination, ignores the contribution of the diffusion current, and also considers balanced electron and hole mobilities. It also ignores any potential barriers and space charge at the interfaces, implying that the open-circuit voltage is equal to the built-in potential ($V_{OC} = V_{bi}$). From this approach, we obtain an analytical relation between the fill factor and θ_o, which reproduces that obtained by Bartesaghi *et al.* [12] based on numerical simulations. We also derive another expression for the coefficient α of the intensity dependence for the short-circuit current, $J_{SC} \propto I$, as a function of θ_o, further demonstrating that α is not simply related to the recombination order, but results from the competition between current extraction and charge recombination within the active layer. The model is applied to an ITO/PEDOT:PSS/P3HT:PC61BM/Ca/Al device, and from the fittings it is obtained how the charge-carrier mobility, the coefficient α, and the dissociation probability P vary with temperature. Therefore, this simple analytical model can be used to extract useful microscopic parameters from experimental J_{ph}-V curves, and to predict the fill factor, the intensity dependence of the photocurrent, and the relative importance of charge extraction and recombination in the measured device.

ACKNOWLEDGMENTS

The authors acknowledge the Brazilian funding Agencies CNPq, CAPES, and FAPESP, and the National Institute for Science and Technology on Organic Electronics (INEO) for the support given to this work.

[1] K. Lehovec, The photo-voltaic effect, Phys. Rev. **74**, 463 (1948).
[2] L. Lu, T. Zheng, Q. Wu, A. M. Schneider, D. Zhao, and L. Yu, Recent advances in bulk heterojunction polymer solar cells, Chem. Rev. **115**, 12666 (2015).
[3] A. Gusain, R. M. Faria, and P. B. Miranda, Polymer solar cells-interfacial processes related to performance issues, Front. Chem. **7**, 61 (2019).
[4] U. Würfel, D. Neher, A. Spies, and S. Albrecht, Impact of charge transport on current-voltage characteristics and power-conversion efficiency of organic solar cells, Nat. Commun. **6**, 6951 (2015).
[5] L. J. A. Koster, M. Kemerink, M. M. Wienk, K. Maturová, and R. A. J. Janssen, Quantifying bimolecular recombination losses in organic bulk heterojunction solar cells, Adv. Mater. **23**, 1670 (2011).
[6] C. M. Proctor, S. Albrecht, M. Kuik, D. Neher, and T. Q. Nguyen, Overcoming geminate recombination and enhancing extraction in solution-processed small molecule solar cells, Adv. Energy Mater. **4**, 1400230 (2014).
[7] B. M. Savoie, B. Movaghar, T. J. Marks, and M. A. Ratner, Simple analytic description of collection efficiency in organic photovoltaics, J. Phys. Chem. Lett. **4**, 704 (2013).
[8] W. Shockley and H. J. Queisser, Detailed balance limit of efficiency of p-n junction solar cells, J. Appl. Phys. **32**, 510 (1961).
[9] D. Gupta, S. Mukhopadhyay, and K. S. Narayan, Fill factor in organic solar cells, Sol. Energy Mater. Sol. Cells **94**, 1309 (2010).

[10] N. A. Ran, J. A. Love, M. C. Heiber, X. Jiao, M. P. Hughes, A. Karki, M. Wang, V. V. Brus, H. Wang, D. Neher, H. Ade, G. C. Bazan, and T.-Q. Nguyen, Charge generation and recombination in an organic solar cell with Low energetic offsets, Adv. Energy Mater. **8**, 1701073 (2018).

[11] S. M. Hosseini, S. Roland, J. Kurpiers, Z. Chen, K. Zhang, F. Huang, A. Armin, D. Neher, and S. Shoaee, Impact of bimolecular recombination on the fill factor of fullerene and nonfullerene-based solar cells: A comparative study of charge generation and extraction, J. Phys. Chem. C **123**, 6823 (2019).

[12] D. Bartesaghi, I. D. C. Pérez, J. Kniepert, S. Roland, M. Turbiez, D. Neher, and L. J. A. Koster, Competition between recombination and extraction of free charges determines the fill factor of organic solar cells, Nat. Commun. **6**, 7083 (2015).

[13] M. C. Heiber, T. Okubo, S.-J. Ko, B. R. Luginbuhl, N. A. Ran, M. Wang, H. Wang, M. A. Uddin, H. Y. Woo, G. C. Bazan, and T.-Q. Nguyen, Measuring the competition between bimolecular charge recombination and charge transport in organic solar cells under operating conditions, Energy Environ. Sci. **11**, 3019 (2018).

[14] M. Stolterfoht, A. Armin, B. Philippa, and D. Neher, The role of space charge effects on the competition between recombination and extraction in solar cells with Low-mobility photoactive layers, J. Phys. Chem. Lett. **7**, 4716 (2016).

[15] D. Neher, J. Kniepert, A. Elimelech, and L. J. A. Koster, A New figure of merit for organic solar cells with transport-limited photocurrents, Sci. Rep. **6**, 24861 (2016).

[16] S. M. Arnab and M. Z. Kabir, An analytical model for analyzing the current-voltage characteristics of bulk heterojunction organic solar cells, J. Appl. Phys. **115**, 034504 (2014).

[17] M. L. Inche Ibrahim, Z. Ahmad, and K. Sulaiman, Analytical expression for the current-voltage characteristics of organic bulk heterojunction solar cells, AIP Adv. **5**, 027115 (2015).

[18] Y. T. Set, T. Zhang, E. Birgersson, and J. Luther, What parameters can be reliably deduced from the current-voltage characteristics of an organic bulk-heterojunction solar cell?, J. Appl. Phys. **117**, 084503 (2015).

[19] W. U. Huynh, J. J. Dittmer, N. Teclemariam, D. J. Milliron, A. P. Alivisatos, and K. W. J. Barnham, Charge transport in hybrid nanorod-polymer composite photovoltaic cells, Phys. Rev. B **67**, 115326 (2003).

[20] J. K. J. van Duren, X. Yang, J. Loos, C. W. T. Bulle-Lieuwma, A. B. Sieval, J. C. Hummelen, and R. A. J. Janssen, Relating the morphology of poly(p-phenylene vinylene)/methanofullerene blends to solar-cell performance, Adv. Funct. Mater. **14**, 425 (2004).

[21] L. Liu, W. E. Stanchina, and G. Li, Effects of semiconducting and metallic single-walled carbon nanotubes on performance of bulk heterojunction organic solar cells, Appl. Phys. Lett. **94**, 233309 (2009).

[22] G. F. a Dibb, T. Kirchartz, D. Credgington, J. R. Durrant, and J. Nelson, Analysis of the relationship between linearity of corrected photocurrent and the order of recombination in organic solar cells, J. Phys. Chem. Lett. **2**, 2407 (2011).

[23] P. Langevin, Recombinaison et mobilites des ions dans les gaz, Ann. Chim. Phys. **28**, 433 (1903).

[24] A. Pivrikas, G. Juška, A. J. Mozer, M. Scharber, K. Arlauskas, N. S. Sariciftci, H. Stubb, and R. Österbacka, Bimolecular Recombination Coefficient as a Sensitive Testing Parameter for Low-Mobility Solar-Cell Materials, Phys. Rev. Lett. **94**, 176806 (2005).

[25] C. G. Shuttle, B. O'Regan, A. M. Ballantyne, J. Nelson, D. D. C. Bradley, J. De Mello, and J. R. Durrant, Experimental determination of the rate law for charge carrier decay in a polythiophene: Fullerene solar cell, Appl. Phys. Lett. **92**, 093311 (2008).

[26] M. C. Heiber, C. Baumbach, V. Dyakonov, and C. Deibel, Encounter-Limited Charge-Carrier Recombination in Phase-Separated Organic Semiconductor Blends, Phys. Rev. Lett. **114**, 136602 (2015).

[27] C. Deibel, A. Wagenpfahl, and V. Dyakonov, Origin of reduced polaron recombination in organic semiconductor devices, Phys. Rev. B **80**, 075203 (2009).

[28] M. Hilczer and M. Tachiya, Unified theory of geminate and bulk electron-hole recombination in organic solar cells, J. Phys. Chem. C **114**, 6808 (2010).

[29] Y. Liu, K. Zojer, B. Lassen, J. Kjelstrup-Hansen, H.-G. Rubahn, and M. Madsen, Role of the charge-transfer state in reduced langevin recombination in organic solar cells: A theoretical study, J. Phys. Chem. C **119**, 26588 (2015).

[30] T. M. Burke, S. Sweetnam, K. Vandewal, and M. D. McGehee, Beyond langevin recombination: How equilibrium between free carriers and charge transfer states determines the open-circuit voltage of organic solar cells, Adv. Energy Mater. **5**, 1500123 (2015).

[31] G. Lakhwani, A. Rao, and R. H. Friend, Bimolecular recombination in organic photovoltaics., Annu. Rev. Phys. Chem. **65**, 557 (2014).

[32] R. D. Pensack and J. B. Asbury, Beyond the adiabatic limit: Charge photogeneration in organic photovoltaic materials, J. Phys. Chem. Lett. **1**, 2255 (2010).

[33] C. L. Braun, Electric field assisted dissociation of charge transfer states as a mechanism of photocarrier production, J. Chem. Phys **80**, 4157 (1984).

[34] C. Deibel, T. Strobel, and V. Dyakonov, Origin of the Efficient Polaron-Pair Dissociation in Polymer-Fullerene Blends, Phys. Rev. Lett. **103**, 036402 (2009).

[35] M. Lenes, M. Morana, C. J. Brabec, and P. W. M. Blom, Recombination-Limited photocurrents in Low bandgap polymer/fullerene solar cells, Adv. Funct. Mater. **19**, 1106 (2009).

[36] S. Tscheuschner, H. Bässler, K. Huber, and A. Köhler, A combined theoretical and experimental study of dissociation of charge transfer states at the donor-acceptor interface of organic solar cells, J. Phys. Chem. B **119**, 10359 (2015).

[37] S. Athanasopoulos, S. Tscheuschner, H. Bässler, and A. Köhler, Efficient charge separation of cold charge-transfer states in organic solar cells through incoherent hopping, J. Phys. Chem. Lett. **8**, 2093 (2017).

[38] L. J. A. Koster, E. C. P. Smits, V. D. Mihailetchi, and P. W. M. Blom, Device model for the operation of polymer/fullerene bulk heterojunction solar cells, Phys. Rev. B - Condens. Matter Mater. Phys. **72**, 085205 (2005).

[39] S. Altazin, R. Clerc, R. Gwoziecki, G. Pananakakis, G. Ghibaudo, and C. Serbutoviez, Analytical modeling of organic solar cells and photodiodes, Appl. Phys. Lett. **99**, 143301 (2011).

[40] L. F. Hernández-García, V. Cabrera-Arenas, and L. M. Reséndiz-Mendoza, On the convergence of the algorithm for simulating organic solar cells, Comput. Phys. Commun. **196**, 372 (2015).

[41] R. Mauer, M. Kastler, and F. Laquai, The impact of polymer regioregularity on charge transport and efficiency of P3HT:PCBM photovoltaic devices, Adv. Funct. Mater. **20**, 2085 (2010).

[42] K. Li, L. Li, and J. C. Campbell, Recombination lifetime of free polarons in polymer/fullerene bulk heterojunction solar cells, J. Appl. Phys. **111**, 034503 (2012).

[43] H. E. Tseng, T. H. Jen, K. Y. Peng, and S. A. Chen, Measurements of charge mobility and diffusion coefficient of conjugated electroluminescent polymers by time-of-flight method, Appl. Phys. Lett. **84**, 1456 (2004).

[44] S. R. Cowan, R. A. Street, S. Cho, and A. J. Heeger, Transient photoconductivity in polymer bulk heterojunction solar cells: Competition between sweep-out and recombination, Phys. Rev. B **83**, 035205 (2011).

[45] See Supplemental Material at http://link.aps.org/supplemental/10.1103/PhysRevApplied.14.034046 for a detailed development of the analytical model as well as simulations showing its validity limits.

[46] R. Courant, Differential & Integral Calculus, (1936).

[47] J. Lorrmann, B. H. Badada, O. Inganäs, V. Dyakonov, and C. Deibel, Charge carrier extraction by linearly increasing voltage: Analytic framework and ambipolar transients, J. Appl. Phys. **108**, 113705 (2010).

[48] D. J. Coutinho, G. C. Faria, D. T. Balogh, and R. M. Faria, Influence of charge carriers mobility and lifetime on the performance of bulk heterojunction organic solar cells, Sol. Energy Mater. Sol. Cells **143**, 503 (2015).

[49] O. Armbruster, C. Lungenschmied, and S. Bauer, Investigation of trap states and mobility in organic semiconductor devices by dielectric spectroscopy: Oxygen-doped P3HT:PCBM solar cells, Phys. Rev. B. **86**, 235201 (2012).

[50] I. Taibi, A. Belghachi, and H. Abid, Effect of trapping and temperature on the performance of P3HT: PCBM organic solar cells, Optik **127**, 8592 (2016).

[51] V. D. Mihailetchi, H. Xie, B. De Boer, L. J. A. Koster, and P. W. M. Blom, Charge transport and photocurrent generation in poly(3-hexylthiophene): Methanofullerene bulk-heterojunction solar cells, Adv. Funct. Mater. **16**, 699 (2006).

[52] P. Schilinsky, C. Waldauf, and C. J. Brabec, Recombination and loss analysis in polythiophene based bulk heterojunction photodetectors, Appl. Phys. Lett. **81**, 3885 (2002).

[53] D. Scheunemann, O. Kolloge, S. Wilken, M. Mack, J. Parisi, M. Schulz, A. Lützen, and M. Schiek, Revealing the recombination dynamics in squaraine-based bulk heterojunction solar cells, Appl. Phys. Lett. **111**, 183502 (2017).

[54] N. Gasparini, A. Wadsworth, M. Moser, D. Baran, I. McCulloch, and C. J. Brabec, The physics of small molecule acceptors for efficient and stable bulk heterojunction solar cells, Adv. Energy Mater. **8**, 1703298 (2018).